Ab initio study of small diameter (6, 6) armchair carbon nanoropes: orientational dependent properties

2003 J. Phys.: Condens. Matter 15 6931

(http://iopscience.iop.org/0953-8984/15/41/003)

INSTITUTE OF PHYSICS PUBLISHING JOURNAL OF PHYSICS: CONDENSED MATTER

J. Phys.: Condens. Matter **15** (2003) 6931–6942 PII: S0953-8984(03)66387-3

Ab initio study of small diameter (6, 6) armchair carbon nanoropes: orientational dependent properties

B K Agrawal, S Agrawal and R Srivastava

Physics Department, Allahabad University, Allahabad 211002, India

Received 18 July 2003
Published 3 October 2003
Online at stacks.iop.org/JPhysCM/15/6931

Abstract

A comprehensive *ab initio* investigation of the effects of the relative orientation (RO) between the adjacent tubes in a rope on the stability, structural, electronic, optical and Raman-active properties has been performed for the ropes of small diameter carbon (6, 6) nanotubes. A number of new features not discussed earlier are observed in the present study. The symmetric rope with an RO of 0° is metallic in all directions, whereas the asymmetric ropes with a non-zero value of RO are semiconductors along the tube axis but semi-metallic normal to rope axis. The band gap increases with RO up to an angle of 15° and thereafter reveals oscillatory behaviour. No dips appear in the symmetric rope but they do exist in the asymmetric rope. Strong optical absorption appears along the axis in the energy range 2.4–4.2 eV in the isolated tube. On the other hand, for the ropes, the strong absorption extends up to the energy region 1.8–4.5 eV. Strong peaks also occur at 0.05 and 0.15 eV for the ropes with RO = 0° and 15°, respectively. The even-parity Raman-active radial breathing mode (RBM) frequencies calculated here for the isolated (n, n), $n = 3$–6 tubes are seen to deviate from the usual $\omega \propto 1/d$ law (where d is the tube diameter). For small diameter tubes, this shows an approximate variation, $\omega = 1/d^{1/2}$. The RBM frequencies for the ropes are either greater or smaller compared to the isolated tube, depending on the value of RO. A cubic anharmonicity of about 14% is seen in the potential for the radial mode vibrations. The RBM frequencies calculated here for some ropes, which are lower compared to that of the isolated tube, concur with the available Raman data.

1. Introduction

Unique properties, such as small diameter, high tensile strength, high chemical and thermal stabilities, and remarkable electronic and heat conduction, are associated with carbon nanotubes, which are candidates for next-generation nano-sized electronic devices. Their quasi-one-dimensional character and the curvature effect give rise to novel features.

0953-8984/03/416931+12$30.00

In one-dimensional systems, critical points at the Γ-point, the Brillouin zone (BZ) boundaries and the saddle points within the BZ lead to square-root-like singularities in the electron density of states (DOS). Such singularities on the top of the ropes of both the armchair and zigzag metallic nanotubes have been seen in scanning tunnelling measurements (Wildoer *et al* 1998, Odom *et al* 1998, 2000). The occurrence of small gaps have been reported by Ouyang *et al* (2001) using scanning tunnelling microscopy. Optical absorption and Raman scattering measurements have thrown light on the electronic structure of nanotubes.

Most of theoretical studies have been performed on isolated wide nanotubes (Hamada *et al* 1992, Mintmire *et al* 1992, Saito *et al* 1992, Lee *et al* 1997, Liu and Chan 2002) and there are only a few efforts on bundles of nanotubes (Charlier *et al* 1995, Low 1997, Kwon *et al* 1998, Delaney *et al* 1998, 1999, Maarouf *et al* 2000, Reich *et al* 2002). Delaney *et al* (1998, 1999) have noted small gaps in the crystalline bundles of (10, 10) nanotubes and reported that the DOS is not changed by the relative orientation of the tubes in a rope. An increase of 7% in the DOS was seen by Kwon *et al* (1998) for the (10, 10) rope crystal over the nanotube. Reich *et al* (2002) have studied the *unrelaxed* (6, 6) nanocrystal. The present work is a detailed *ab initio* study of the structural, vibrational, electronic and optical properties of a comparatively small diameter (6, 6) tube in isolation, as well as their nanoropes, considering full optimization.

This study is motivated by a number of factors. The following questions have not been addressed until now. Firstly, there are no reports available in the literature for ropes of (6, 6) tubes with an RO of more than 10°. The present study extends the study up to RO = 45°. Secondly, the available report by Reich *et al* (2002) for unrelaxed (6, 6) ropes is not reliable because of the inherent forces in the unrelaxed geometries of the ropes. Thirdly, no *ab initio* calculation for optical absorption for the (6, 6) nanoropes is available in the literature. Next, the difference in the Raman-active radial breathing mode (RBM) frequencies between the isolated (6, 6) nanotube and the ropes of the (6, 6) nanotubes needs to be known, as the Raman data for wide tubes observed by Rao *et al* are not well explained by theory. The behaviour of the optical absorption and the Raman-active modes may be used to identify small diameter achiral armchair nanotubes and ropes. The usual inverse frequency law, $\omega_{\mathrm{RBM}} \propto 1/d$ (where d is the diameter of the tube), for the RBM frequency needs to be tested in the small diameter limit. This paper addresses all the above questions.

2. Method and technical details

Calculations have been performed in a self-consistent manner using the ABINIT code[1], which uses the pseudopotential and plane waves along with density functional theory. An efficient fast Fourier transform algorithm (Goedecker 1997) is used for the conversion of wavefunctions between the real and reciprocal lattices. The wavefunctions are determined in a fixed potential according to a state-by-state or band-by-band conjugate gradient algorithm (Payne *et al* 1992, Gonze 1996). A self-consistent potential is determined by using a potential-based conjugate gradient algorithm. We consider a soft non-local pseudopotential (Troullier and Martins 1991) within a separable approximation (Kleinman and Bylander 1982) and use the exchange–correlation potential (Perdew *et al* 1996) in the generalized gradient approximation (GGA) generated by FHI (Fritz Haber Institute) code (Fuchs and Scheffler 1999).

All the structures have been optimized to achieve minimum energy by relaxing both the lattice constants and the atomic positions in the unit cell simultaneously. It may be pointed out that the magnitude of atomic relaxation depends on the plane-wave cut-off energy and that one should obtain convergence with respect to the cut-off energy too.

[1] The ABINIT code is a common project of the Université catholique de Louvain, Corning Inc and other contributors.

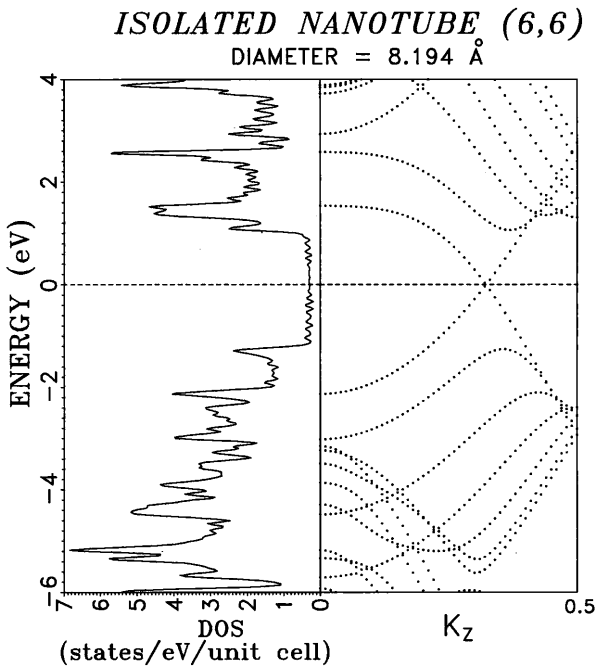

Figure 1. The electronic structure and density of electron states in the vicinity of the Fermi level for the isolated (6, 6) nanotube.

All the calculations have been performed in a self-consistent manner. The structures studied have been optimized for Hellmann–Feynman forces as small as 10^{-2} eV Å^{-1} on each atom. Sufficient vacuum space has been chosen to avoid the interference effects between the neighbouring isolated nanotubes in supercell geometries. A cut-off energy of 60 Ryd for the plane-wave basis has been seen to be sufficient for achieving convergence. Convergence with respect to the number of k-points in the BZ has also been tested.

3. Calculation and results

3.1. Isolated (6, 6) nanotube

3.1.1. Stability and structure. In order to check the present results with some of those of earlier workers available for isolated nanotubes, we firstly investigate the (6, 6) isolated tube. To calculate the binding energy (BE) per atom, we determine the tube energy per atom of the unit cell and subtract it from the energy of the isolated carbon atoms. This calculated energy is named the BE per atom.

One observes an increase in BE with the diameter of the tube. The enhancements in the BEs of the (6, 6) tube over the (3, 3), (4, 4) and (5, 5) nanotubes are seen to be 366, 152 and 53 meV, respectively. It is thus noted that the stability of a nanotube increases with diameter quite rapidly for small diameter tubes but slowly for wide nanotubes. The diameter of the isolated (6, 6) nanotube is 8.194 Å. The C–C bond lengths within the plane or between the carbon atoms lying in the adjacent planes are equal and are 1.422 Å.

3.1.2. Electronic structure. The electronic structure and electron DOS for the (6, 6) tube are presented in figure 1. The origin of the energy has been chosen to be the Fermi level (E_F).

Both the electronic structure and the DOS have been computed for 51 k-points along the tube axis with a broadening of 0.055 eV. The width of the valence band below E_F is 19.76 eV. The separation (ΔE) between the two van Hove singularities around E_F is 3.66 eV, which is in agreement with that of Reich *et al* (2002).

A perusal of the DOS in figure 1 reveals that the DOS in the neighbourhood of E_F is equal to 0.29 states eV^{-1}/unit cell. The saddle points lying on both sides of E_F in the conduction and valence band regions determine the occurrence of the peaks forming the plateau in the DOS.

3.1.3. Optical absorption. We calculate the zero-phonon optical absorption spectra of the isolated nanotube and its ropes by using the absorption coefficient (Hybertson and Needles 1993) as

$$\alpha(\omega) = \frac{4\pi^2 e^2}{ncm^2\omega V_c} \sum_{v,c,\vec{k}} |\vec{\varepsilon} \cdot \vec{p}_{cv}(\vec{k})|^2 \delta(E_c - E_v - \hbar\omega) \tag{1}$$

where m and e are the electron mass and charge, c is velocity of light, n is the refractive index, V_c is the unit cell volume including the empty space, and $\vec{\varepsilon}$ denotes a unit electric vector of the polarized incident light. E_c and E_v are the conduction and valence state energies and $\hbar\omega = (E_c - E_v)$. The momentum matrix element $\vec{p}_{cv}(k)$ for the wavevector $\vec{k}$ is given by

$$\vec{p}_{cv}(\vec{k}) = \langle \psi_c, \vec{k} | \vec{p} | \psi_v, \vec{k} \rangle \tag{2}$$

where ψ_c and ψ_v denote the wavefunctions of the conduction and the valence states, respectively, and $\vec{p}$ is the momentum operator.

In the actual calculation, for simplicity we consider the polarization of light confined in one direction, x, y or z, as well as $n = 1$. A higher value of n will reduce the overall intensity accordingly.

The no-phonon absorption for the (6, 6) single tube along and normal to the direction of the tube axis has been presented in figure 2(a). Strong peaks appear at 2.35 ± 0.20, 2.65 ± 0.1, 2.95 ± 0.1 eV and in the region 3.4–4.25 eV. The strong peaks in the region 2.35 ± 0.20 eV arise from the transitions between the occupied states 46 and 47 and the unoccupied states 50 and 51 at $k_z = 0.32$–0.40. The strongest peak at 3.4 eV appears because of the transition between the occupied states 44–47 and the unoccupied states 49–52 at $k_z = 0.44$ etc.

The optical absorption normal to the tube axis is very weak and concurs with the measured data of Hwang *et al* (2000) and Li *et al* (2001), who have measured practically zero absorption for the nanotubes.

3.1.4. Vibrational frequencies. It is known that the even-parity A_{1g} RBM is not sensitive to nanotube structure but to the nanotube radius. After employing a frozen phonon approximation, we have calculated the RBM frequency for the isolated tubes, which can be measured by Raman measurements. We study the variation of system energy with the very small displacements of atoms in the radial direction of the nanotubes. To evaluate the harmonic and cubic anharmonic force constants, we have fitted the variation of the system energy with a polynomial containing terms up to third order. These force constants are determined at the minimum system energy where the forces on each atom vanish. The computed RBM frequencies for the isolated (n, n) tubes for $n = 3$–6 are 532, 472, 445 and 402 cm^{-1}, respectively. For the isolated (3, 3) nanotube, the RBM frequency appearing at 532 cm^{-1} is quite close to a Raman peak measured at 534 cm^{-1} by Tang *et al* (1998), Sun *et al* (1999) and Wang *et al* (2001) in single-wall nanotubes with diameters smaller than 7 Å. Liu and Chan (2002) have also obtained a value of 538 cm^{-1} for the (3, 3) tube, which is quite close to ours, after employing a simple harmonic oscillator problem.

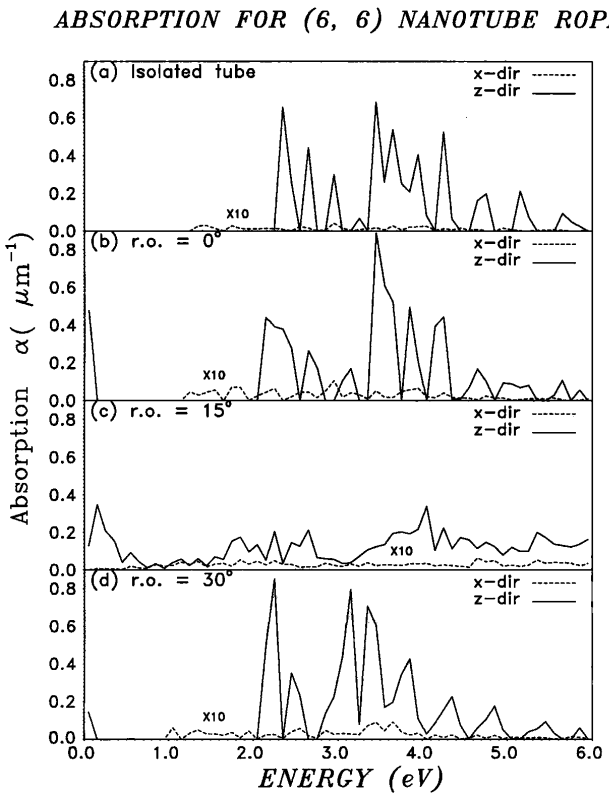

Figure 2. Absorption spectra in the energy region 0–6.0 eV for (a) the isolated (6, 6) nanotube and for various ropes with relative orientation between adjacent tubes equal to (b) 0°, (c) 15° and (d) 30°.

The RBM frequency decreases with the diameter of the nanotube. The variation of frequency with tube diameter does not obey the usually accepted variation (Kurti *et al* 1998), i.e. the frequency is inversely proportional to the diameter of the nanotube. In contrast, we obtain a variation near to $\omega = 1/d^{1/2}$. This type of variation should be observable in Raman measurements for the ultra-thin and medium-sized diameter nanotubes.

3.2. Nanoropes

3.2.1. Structural properties. We constructed the ropes or bundles of the nanotubes by repeating the single nanotube along a hexagonal periodic lattice in the plane normal to the tube axis. For the optimization, we consider all three lattice constants: one along the tube axis and two for the hexagonal lattice in the k_x–k_y plane as well as all the atomic positions of the unit cell. One of the hexagonal axes passes through the mid-point of the two atoms lying in one plane. Different types of ropes were created by rotating each nanotube by different angles. A rope is then designated by the amount of RO between the two nearest-neighbouring nanotubes. We have investigated the ropes with RO in the range 0°–60°. The BE for the (6, 6) rope, similarly to the (3, 3) rope (Agrawal *et al* 2003), decreases with RO up to an angle of 30°.

For a more precise discussion of the relative stability of the nanoropes, one should at least consider the zero-point vibrational energy and the vibrational partition function, which is beyond the scope of this study.

We now look into the variation of the size of the unit cell of a rope in various directions with RO. It is seen that all the ropes studied whose structures have been optimized for minimum energy have different sizes of unit cell along the axis of the constituent nanotubes (a_Z). The values of a_Z are 2.45, 2.51 and 2.38 Å for RO equal to 0°, 15° and 30°. The values of the lattice constants a_x and a_y normal to the rope axis are equal ($a_x = a_y$). The unit cell retains more or less its perfect hexagonal character. We find that the unit cell sizes in the x or y directions (a_x and a_y) change with RO. The values of a_x ($=a_y$) are 12.04, 12.00 and 12.26 Å for RO equal to 0°, 15° and 30°, respectively. The mean diameters for the ropes containing RO equal to 0°, 15° and 30° are 8.23, 8.06 and 8.38 Å, respectively. The 15° rope has minimum diameter.

Variations in the C–C bond lengths in a nanotube of a rope are seen with RO. Let $r_\parallel$ denote the bond length between the carbon atoms lying in the adjacent planes of the hexagonal unit cell and $r_\perp$ the bond length within a single plane. An irregular behaviour in the value of $(r_\perp - r_\parallel)$ is seen for the (6, 6) ropes. The difference $(r_\perp - r_\parallel)$ is 1.2% for RO = 0°, 5.2% for RO = 30° and −2.8% for RO = 15°.

The values of the minimum separation between the atoms lying on the two adjacent nanotubes in a rope are 3.81, 3.93 and 3.87 Å for the ropes with RO equal to 0°, 15° and 30°, respectively.

3.2.2. Electronic structure. The (6, 6) nanotubes with zero RO between neighbouring tubes are quite symmetric because the structure possesses six-fold symmetry along the vertical z direction, the symmetric vertical mirror planes containing the tube axis, and the two-fold axis along the x-axis. The point group symmetry is D_{6h}. This symmetry gives rise to the crossing of bonding and anti-bonding states at E_F, making it metallic. This symmetry is also compatible with the hexagonal lattice of the rope. A rope containing non-zero RO between the two nearest tubes loses D_{6h} symmetry and becomes non-symmetrical. In fact, the point group symmetry is reduced to C_{6h}, where symmetric vertical planes no longer exist. This should induce a gap in the electronic structure in the neighbourhood of E_F in all the ropes.

0° *rope.* The electronic structures and DOS for 51 k-points along the tube axis for RO = 0° in a rope are presented in figure 3. The zero band gap is retained in the rope and the rope remains metallic. A comparison of the electronic structures of the isolated and symmetric ropes reveals that the overall electronic structure remains the same. The widths of the valence bands are exactly the same. Very small changes in the state energies are seen in the lower part (below −6 eV) of the valence band. Similarly, two saddle points appearing in the $k_z = 0.42$–0.44 range (below and above E_F) have an energy interval of 2.2 eV in the rope similar to the isolated tube. However, appreciable changes are observed in the neighbourhood of E_F. In particular, the separation (ΔE) between the two critical points at the Γ-point nearest to E_F is 3.35 eV, in contrast to the value of 3.66 eV seen in the isolated tube. The bonding and anti-bonding states in the rope now cross at a slightly increased value of $k_z = 0.32$. The nearly constant DOS around E_F increases in the rope and the value is 0.36 states eV^{-1}/unit cell, compared to 0.29 for the isolated tube. An increase of ∼24% in DOS at E_F is observed in the rope. This result is in agreement with the conclusion of Kwon *et al* (1998), who observed an increase of 7% in the DOS in the (10, 10) nanorope over the (10, 10) nanotube.

The electronic structure for the (6, 6) ropes reveals that ΔE shows a regular increase with RO. The values of ΔE are 3.35 and 3.23 eV for ROs of 0° and 15°, in contrast to a value of 3.66 eV for the isolated tube. The present reduction in ΔE in a rope for RO < 15°, compared to the isolated tube, is in agreement with the observation of Reich *et al* (2002). The valence bandwidth for the various (6, 6) ropes remains practically constant, equal to 19.97 eV, for the various values of RO. The present results and those of Reich *et al* for the (6, 6) tube and rope

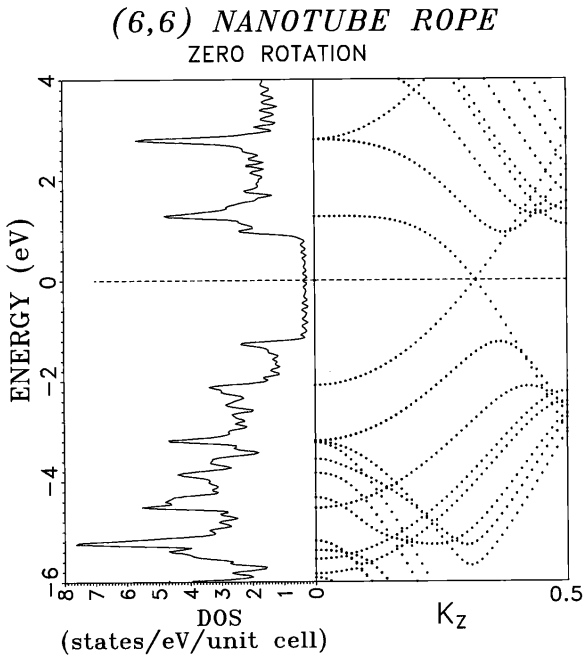

Figure 3. As for figure 1, but for the symmetric nanorope containing adjacent nanotubes with zero relative orientation.

are in disagreement with the conclusion of Rao *et al* (2001), who observed an increase in ΔE in the ropes of wide tubes, in contrast to the present result of a reduction in ΔE. The above discrepancy arises because both the calculations (ours and Reich *et al*) are first-principles calculations whereas Rao *et al* used a parametrized calculation of Kwon *et al* (1998), who considered the tight-binding parametrization assuming pairwise interactions describing both the closed-shell interatomic repulsion and the long-range attractive van der Waals interaction. In a careful LDA or GGA calculation, one studies all types of interactions, and extra arbitrary interactions are not warranted. Quite similar observations have been made by Reich *et al* about the conclusions of Rao *et al* (see the reference for more details). It does not need to be emphasized that the *ab initio* calculations are preferred over the parametrized calculations, for obvious reasons. Kwon *et al* have appreciated this fact in their work by comparing the results obtained by parametrized calculations with those of the *ab initio* results at various steps of their study.

The rope, which is infinitely extended here in all three dimensions in the present calculation, will also have electronic dispersion normal to the tube axis. The dispersion at the crossing point Δ_F obtained along the tube axis in the k_x–k_y plane along symmetry directions is shown in figure 4(a). The two symmetry points in the k_x–k_y plane are chosen to be P (0, 0.5, Δ_F) and U (0.29, 0.375, Δ_F). For the relaxed rope, one observes a small dispersion up to a maximum of 0.39 eV in the k_x–k_y plane along the $P \rightarrow U$ boundary of the BZ. The present result for the relaxed rope is in sharp contrast to the corresponding value of 0.6 eV reported by Reich *et al* (2002), who obtained this value for the *unrelaxed* rope.

In order to fully understand the electronic structure of the three-dimensional structure of the rope, we have performed self-consistent calculations for the band structure along several lines in the z direction (along the tube axis) at several non-zero values of k_x and k_y. In the

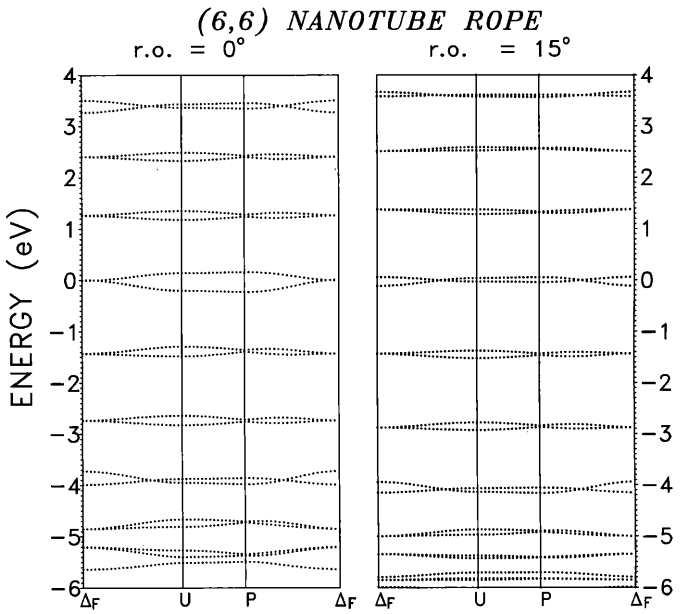

Figure 4. Dispersion in the electronic structure in a plane normal to the nanotube axis in the symmetric (a) RO = 0° and (b) RO = 15° rope along the symmetry directions.

absence of tube–tube interactions, one may expect the band structure to be identical along each line and similar to that of an isolated nanotube where bonding and anti-bonding bands cross E_F linearly. The crossing of the bands along the different lines appears at different values of k_z. We observe a variation in the value of E_F along the different lines, and one should average the various E_Fs. It is also seen that the location of the crossing point is line-dependent. The energy of the crossing point for the different lines must be determined with respect to the averaged E_F. For each line, the crossing point lies, in general, below E_F or above E_F. The calculated DOS along these different lines is similar to that of the $k_x = k_y = 0$ line and is non-zero at E_F. The rope is thus metallic along all the lines parallel to the tube axis. This conclusion is in contrast to that of Delaney *et al* (1999), who obtained band gaps along most lines for the symmetric (10, 10) rope.

In the k_x–k_y planes lying at different values of k_z, in general large band dispersions appear. However, in the vicinity of the crossing of the bonding and the anti-bonding states in the range $k_z = 0.27$–0.29, these dispersions are reduced. The calculated DOS reveals an appreciable DOS in the vicinity of E_F, supporting the metallic character of the rope normal to its axis. The rope is metallic in all directions.

15° *rope.* As a typical case for a rope with a non-zero value of RO between the adjacent tubes, we now discuss the rope containing tubes with RO equal to 15°. The electronic structure and the DOS for the wavevectors along the tube axis are shown in figure 5. One observes a splitting in the degenerate states both in the valence and conduction band regions. This results in a more spiky structure in the DOS. A gap of 79 meV appears at $k_z \approx 0.30$, named Δ_F. A pseudo-gap is seen in the DOS and the minimum value of DOS is 0.04 states eV^{-1}/unit cell. The average DOS outside the pseudo-gap region is 0.33 states eV^{-1}/unit cell.

Figure 4(b) depicts the electronic dispersion in the k_x–k_y plane for RO equal to 15° along symmetry directions of the hexagonal BZ of the rope near Δ_F. A band gap of about 0.172 eV

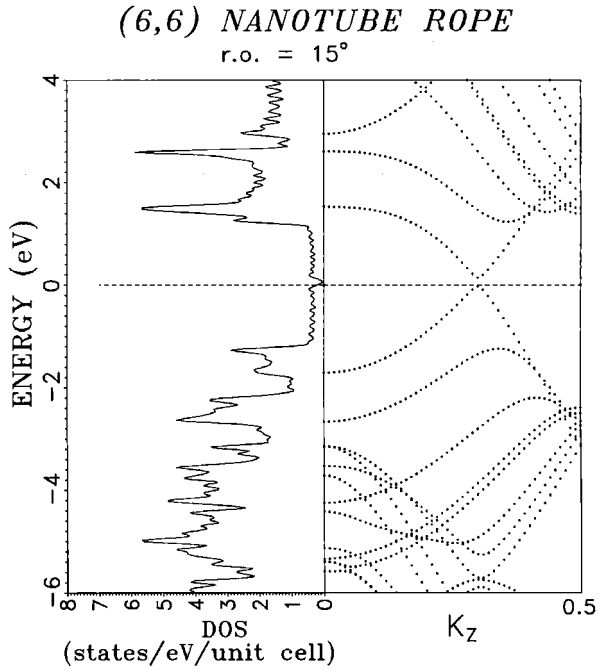

Figure 5. As for figure 1, but for an asymmetric rope containing adjacent nanotubes with a relative orientation of 15°.

is seen at Δ_F, which is much larger than the calculated gap of about 0.079 eV along the k_z direction. In fact, the calculation of dispersions normal to the k_z axis needs a very large number of k-points, both in the k_z and k_x–k_y directions, which we have avoided. The large band gap at Δ_F is a consequence of this limitation. Along the Δ_F–P or Δ_F–U symmetry direction, a decrease in the band gap occurs up to a value as small as 7 meV, which makes the rope semi-metallic in the plane normal to the tube axis. We have performed self-consistent calculations for the electronic structure and the DOS for a number of lines parallel to the tube axis for $k_x \neq 0$ and $k_y \neq 0$ and observed that, along some lines, the band gap is very small and the DOS exhibits appreciable DOS in the vicinity of E_F. Thus, the ropes with a non-zero value of RO are semiconducting along the tube axis but are semi-metallic normal to the tube axis, revealing anisotropic conductivity behaviour.

The calculated pseudo-gap for the (6, 6) ropes are 0, 59, 79, 0 and 65.4 meV for ROs of 0°, 10°, 15°, 30° and 45°, respectively. The calculated band gap for different values of RO shows an oscillating behaviour with a period of 30°. Reich *et al* (2002) have obtained a band gap of 51 meV for the *unrelaxed* (6, 6) rope possessing tubes, each rotated by an angle of 5°, i.e. equivalent to RO = 10° in our notation.

In the above discussion we have investigated minimum-energy-optimized infinitely sized nanorope crystals, which contain an infinite number of tubes. In practice, the length of a real rope ($\approx\mu$m) may reasonably be assumed to approach an infinite length. However, the dimension of the rope normal to its rope axis is finite. Only a rope containing a small number of tubes can be dealt using with the currently available computation facilities. One expects quantum-confined behaviour for ropes of finite diameters. The separation between the electron states and the band gap will be determined by the diameter of the rope. A rope of finite-sized diameter is, in general, expected to be semiconducting normal to the rope axis.

As the calculation for the finite-sized (6, 6) rope is non-trivial, we have performed self-consistent calculations for two finite-sized (3, 3) ropes containing four and seven nanotubes, respectively, with full optimization of the parameters. For a four-tube rope, we observe that the number of bonding and anti-bonding states crossing E_F has increased four-fold. Also, a number of peaks appear in the DOS in the vicinity of E_F. As expected, the rope is thus metallic along the rope axis. The states normal to the rope axis are now quantized and quite small dispersion is seen in these states. The states are well separated. The rope is thus semiconducting normal to the rope axis. Similar results are obtained for the seven-tube rope, except for an increased number of branches crossing E_F. The inter-state separation would decrease with an increase in the number of tubes in a rope, and the rope should remain semiconducting normal to its axis until the inter-state separation reaches a quasi-continuous value. It may be noted that an *ab initio* self-consistent study of a rope containing a large number of tubes is not feasible with the currently available computation facilities.

Further, in actual ropes one will observe disturbances in the periodicity as well as in the relative orientations of the constituent nanotubes. This will lead to a smearing of the Fermi surface.

3.2.3. Optical absorption. The optical absorption for the (6, 6) nanorope for RO $= 0°$ is shown in figure 2(b). Strong peaks appear at 0.05 and 4.2 eV and in the energy ranges 2.05–2.85 and 3.45–4.0 eV. The peak at 0.05 eV arises from the transition between the bonding and the anti-bonding pair near E_F at $k_z = 0.3$. The peaks in the energy range 2.05–2.85 eV originate from the transitions between the occupied states 46 and 47 and the unoccupied states 49–51 in the k_z range of 0.30–0.42. Other peaks arise from the combinations of the states 40–48 with the states 49–56 at $k_z = 0.34$–0.50.

The optical absorption for the (6, 6) nanorope for RO $= 15°$ is shown in figure 2(c). The absorption is seen throughout the energy region. Peaks appear at 0.15, 1.8, 2.3, 2.65, 3.95 ± 0.1 eV and above. The strong peak at 0.15 eV originates from the transitions between the bonding and the anti-bonding pair 48 and 49 at $k_z = 0.3$. Other peaks in the energy range 1.8–2.65 eV originate from the transitions between the occupied states 46 and 47 and the unoccupied states 50 and 51 at $k_z = 0.32$–0.36. The remaining peaks are produced from the transitions between the occupied states 42–48 and the unoccupied states 49–54 at $k_z = 0.34$–0.50.

The optical absorption for the (6, 6) nanorope for RO $= 30°$ is shown in figure 2(d). Strong peaks appear at 2.25 ± 0.2, 2.5 ± 0.1, 3.15 ± 0.15, 3.4 ± 0.1 and 3.8 eV. The strong peaks at 2.25 and 2.5 eV originate from the transitions between the occupied states 46–48 and the unoccupied states 50–52 at $k_z = 0.36$–0.40. Other peaks are produced from transitions between the occupied states 39–48 and the unoccupied states 49–59 at $k_z = 0.40$–0.50.

To sum up for optical absorption, one observes that the strong absorption is mainly seen in the energy region 1.8–4.5 eV. Strong peaks occur at 0.05 and 0.15 eV for the ropes possessing RO $= 0°$ and 15°, respectively.

3.2.4. Vibrational frequencies. The computed RBM frequencies for the (6, 6) nanoropes are 396, 422 and 375 cm^{-1} for RO equal to 0°, 15° and 30°, respectively, showing irregular behaviour with RO. These values correspond to the diameters of the tubes in the rope. The values of ω for the 0° and 30° ropes are lower than that of isolated tube because the diameters of the tubes in the ropes are greater than that of the isolated tube. The reverse is true for the 15° rope. This down-shifting of ω in the bundles has been observed by Rao *et al* (2001) for the ropes of wide tubes. However, they interpreted the Raman data on the basis of the parametrized calculations in a different manner.

4. Conclusions

The energy separation ΔE between the two critical points at the Γ-point near E_F decreases in ropes for RO less than 15° compared to the isolated tube. This is in agreement with the observation of Reich *et al* (2002) but in disagreement with the conclusions of Kwon *et al* (1998) and Rao *et al* (2001), who observed an increase in ΔE. The symmetric rope is metallic in all directions, and the asymmetric rope (with RO $\neq 0$) is semiconducting along the axis but reveals semi-metallic behaviour normal to the axis.

The band gap for the rope increases up to an RO of 15° (79 meV). In the asymmetric rope, we also observe a dip in the DOS, called a pseudo-gap, at E_F. Further, for the (6, 6) *symmetric rope*, we do not find a dip in the DOS at E_F. This is in disagreement with Delaney *et al* (1998, 1999), who saw a pseudo-gap in the symmetric (10, 10) nanorope. However, our results are in agreement with Kwon *et al* (1998).

For the isolated tube along the tube axis, a strong absorption is observed at 2.35 ± 0.15, 3.0 and 3.4 eV. There is no appreciable calculated absorption normal to the tube axis, in agreement with earlier workers (Hwang *et al* 2000, Li *et al* 2001). The strong absorption is seen mainly in the energy region 1.8–4.5 eV. Strong peaks occur at 0.05 and 0.15 eV for the rope possessing RO = 0° and 15°.

We have calculated the frequencies of the even-parity A_{1g} RBM for the isolated (n, n) tubes for $n = 3$ and 6 and also for the different types of (3, 3) ropes. The calculated RBM frequency is 402 cm^{-1} for the isolated tube. The currently calculated RBM frequencies for the isolated (n, n), $n = 3$–6 tubes are not inversely proportional to the diameter of the tubes, as seen earlier for the wide tubes, but shows an approximate variation of $\omega = 1/d^{1/2}$. For the ropes, the calculated RBM frequencies 396 and 375 cm^{-1} are lower than that of the isolated tube and are in agreement with the Raman data of Rao *et al* (2001).

Acknowledgments

The authors express thanks to the University Grants Commissions, New Delhi for financial assistance and to Dr P S Yadav for providing the computation facilities.

References

Agrawal B K, Agrawal S and Srivastava R 2003 *Preprint* (CMPRL/1/2003)
Charlier J C *et al* 1995 *Europhys. Lett.* **29** 43
Delaney P *et al* 1998 *Nature* **391** 466
Delaney P *et al* 1999 *Phys. Rev.* B **60** 7899
Fuchs M and Scheffler M 1999 *Comput. Phys. Commun.* **119** 67
Goedecker S 1997 *SIAM J. Sci. Comput.* **18** 1605
Gonze X 1996 *Phys. Rev.* B **54** 4383
Hamada N *et al* 1992 *Phys. Rev. Lett.* **68** 1579
Hwang J *et al* 2000 *Phys. Rev.* B **62** R13310
Hybertson M S and Needles M 1993 *Phys. Rev.* B **48** 4608
Kleinman L and Bylander D M 1982 *Phys. Rev. Lett.* **48** 1425
Kurti J, Kresse G and Kuzmany H 1998 *Phys. Rev.* B **58** 8869
Kwon Y K, Saito S and Tomanek D 1998 *Phys. Rev.* B **58** R13314
Lee Y H *et al* 1997 *Phys. Rev. Lett.* **78** 2393
Li Z M *et al* 2001 *Phys. Rev. Lett.* **87** 127401
Liu H J and Chan C T 2002 *Phys. Rev.* B **66** 115416
Low J P 1997 *Phys. Rev. Lett.* **79** 1297
Maarouf A A, Kane C L and Mele E J 2000 *Phys. Rev.* B **61** 11156
Mintmire J W *et al* 1992 *Phys. Rev. Lett.* **68** 631

Odom T W *et al* 1998 *Nature* **391** 62
Odom T W *et al* 2000 *J. Phys. Chem.* B **104** 2794
Ouyang M *et al* 2001 *Science* **292** 702
Payne M C *et al* 1992 *Rev. Mod. Phys.* **64** 1045
Perdew J P, Burke K and Ernzerhof M 1996 *Phys. Rev. Lett.* **77** 3865
Rao A M *et al* 2001 *Phys. Rev. Lett.* **86** 3895
Reich S, Thomson C and Ordejon P 2002 *Phys. Rev.* B **65** 155411
Saito R *et al* 1992 *Appl. Phys. Lett.* **60** 2204
Sun H D *et al* 1999 *Solid State Commun.* **109** 365
Tang Z K *et al* 1998 *Appl. Phys. Lett.* **73** 2287
Troullier N and Martins J L 1991 *Phys. Rev.* B **43** 1993
Wang N *et al* 2001 *Nature* **408** 50
Wildoer J W G *et al* 1998 *Nature* **391** 59